

3. NONLINEAR OPTICS FOR QUANTUM FREQUENCY CONVERSION

A working definition for quantum frequency conversion (QFC) is the translation of a quantum state of light from one frequency band to another. First discussed explicitly in the literature nearly 25 years ago by Kumar and colleagues [1,2] in the context of making a tunable source of squeezed light, QFC may play an important role in photonic quantum information processing networks as an interface to link different components (operating at different wavelengths) together. One application would be to map the emission from a single quantum emitter (e.g., InAs/GaAs quantum dots, single neutral alkali atoms, or nitrogen vacancy centers in diamond) to the 1550 nm telecommunications band, for which single mode silica optical fibers show their lowest attenuation levels, and back to the original wavelength for interaction with another single quantum emitter [3]. A second application is in detection, by translating the wavelength of a quantum state for which detection is currently difficult (e.g., due to limitations in detector quantum efficiency, timing resolution, dark count rates, etc.) to one in which high performance detectors have already been developed [4]. More generally, complete and efficient spectro-temporal control of quantum states of light would in principle allow arbitrary quantum photonic components, individually optimized to achieve a desired functionality, to be linked together as part of a high performance quantum internet [5].

In this section, we briefly discuss the fundamentals of QFC in second- and third-order nonlinear media, review the current status of the frequency conversion devices, and highlight recent experiments demonstrating frequency conversion of single photon states of light. Finally, we discuss some perspective towards future directions with QFC, including recent progress using integrated device platforms and proposals for achieving temporal wavepacket shaping using QFC.

3.1 Second-order nonlinear media

Nonlinear media governed by the second-order electronic susceptibility $\chi^{(2)}$ can be used for sum- and difference-frequency generation, in which an input signal at frequency ω_i is combined with a strong pump at frequency ω_p to generate light at the sum and difference frequencies $\omega_o = \omega_i \pm \omega_p$. Because optical nonlinearities are weak, efficient conversion only occurs over an interaction region that is many wavelengths in length. This places the requirement of phase-matching in a pre-eminent position; that is, for efficient sum- or difference-frequency generation, the wavevectors of the three fields must satisfy $\mathbf{k}_o = \mathbf{k}_i \pm \mathbf{k}_p$. While trivial to achieve in vacuum, in solid materials this relationship is almost never satisfied in general because materials exhibit dispersion, that is, the speed of light is wavelength-dependent within the material. Without phase matching, energy oscillates between the three waves involved in the mixing process rather than being monotonically transferred to the output field, and the overall conversion efficiency is low, as in the original second harmonic generation experiment of Peter Franken and co-workers in 1961 [6].

Improvements in conversion efficiency were initially gained using birefringent phase-matching, which takes advantage of the fact that orthogonally polarized light beams travel at different velocities within a birefringent material. By tuning the angles of the input beams appropriately, phase matching can be achieved, although the interaction regions may be limited in size, particularly if tight focusing of the beams is used (which is often the case in order to achieve high intensities). As a result, efficient conversion (on the order of tens of percent) is typically not achieved in these systems without the application of extremely high pump powers.

A development that has increased the utility of frequency conversion devices and been particularly beneficial to subsequent QFC experiments is the use of quasi-phase-matching in a waveguide-based geometry [7]; see Fig 3.1(a). In quasi-phase-matching, the sign of the nonlinear susceptibility is periodically inverted, with the period chosen to match the coherence length. This coherence length is the distance over which the waves

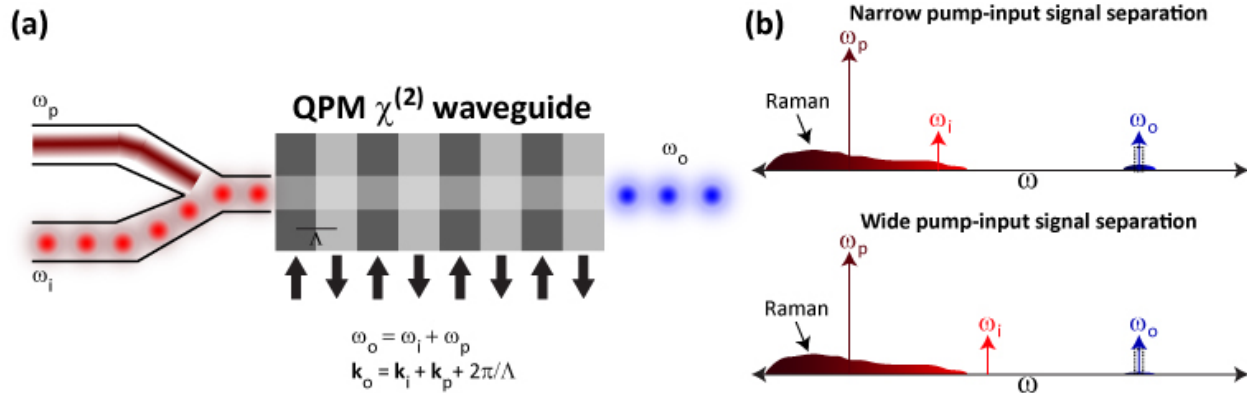


Fig. 3-1. (a) Schematic for quasi-phase-matching (QPM) in a $\chi^{(2)}$ waveguide (here, sum-frequency generation is shown). An input signal at frequency ω_i is combined with a strong pump at frequency ω_p to generate an output signal at ω_o . Phase matching is achieved through periodic poling, which generates a grating momentum $2\pi/\Lambda$ that compensates for wavevector mismatch. (b) The strong pump field can generate broadband Raman scattering in the QPM material. If this Raman scattered light reaches the input signal frequency, it will be frequency converted along with the signal and will thus be a limiting noise source. This source of noise can be limited by: (1) Placing the input signal on the anti-Stokes (higher frequency) side of the pump; (2) Increasing the pump-input signal separation as much as possible; (3) Narrowband spectral filtering around the target conversion frequency.

involved in the mixing process accumulate a relative phase shift of π , so that at longer distances energy would otherwise be transferred back from the output frequency to the input field. Flipping the sign of the nonlinearity at every coherence length ensures that energy will continue to be transferred from input field to output field, albeit at a slower rate than it does in the case of perfect birefringent phase-matching. In momentum space, this is equivalent to saying that the periodic inversion of the nonlinear susceptibility creates an effective grating whose momentum compensates for wavevector mismatch between the three fields involved in the mixing process. Finally, the use of the waveguide geometry provides both a relatively large intensity for the three fields and a long interaction length. Taken altogether, conversion efficiencies (not including input/output coupling losses) in excess of 80% have been achieved for both frequency upconversion and downconversion [8,9].

Periodically-poled lithium niobate (PPLN) waveguides are perhaps the most common devices that have been used in QFC experiments to this point. While theoretically, sum- and difference-frequency generation can be noise-free, suitable for QFC all the way down to the level of single photon Fock states, in practice, one might expect that scattering and fluorescence processes associated with the interaction of a strong pump field with a solid material might lead to significant noise contributions. Raman scattering can be a dominant noise source if the pump and input signal are within a couple hundred nanometers of each other [7]. Keeping the pump on the long-wavelength side of the input signal [7] and increasing the pump-signal separation to several hundred nanometers [8,10] can increase signal-to-noise levels to >100:1 (Fig. 3-1(b)). Spontaneous parametric downconversion can also be of concern, and can be exacerbated due to fabrication errors in the poling process [9].

The first experimental demonstration of QFC using a non-classical input signal was performed by Huang and Kumar [2] soon after Kumar introduced the concept [1], with non-classical intensity correlations between a pair of fields shown to be preserved after one of the fields was frequency converted. Over a decade later, Tanzilli and colleagues [3] showed that entangled fields remain so after one of the fields is frequency converted. This work using non-classical fields came at approximately the same time that several groups began pushing the conversion efficiency levels achievable in $\chi^{(2)}$ nonlinear crystals towards 100%, for applications such as low light level detection of telecommunications-band photons using visible wavelength single photon counters [4,7].

In recent years, a number of experiments have looked at frequency upconversion of single photon Fock states using quasi-phase-matched $\chi^{(2)}$ nonlinear crystals (Fig. 3-2). For example, one experiment combined a 1300 nm triggered

single photon source based on an InAs/GaAs quantum dot with a 1550 nm pump in a PPLN waveguide to generate 710 nm photons, with antibunched photon statistics measured to explicitly confirm the single photon nature of the upconverted light [11]. The utility of frequency conversion for studying the dynamics of telecommunications-band single quantum emitters was also highlighted, where conversion to the visible improved the dynamic range of time-correlated single photon counting measurements of the quantum dot excited state lifetime by a factor of 25, due to the superior characteristics of Si single photon counters (sensitive at 710 nm) relative to InGaAs devices (sensitive at 1300 nm). Subsequent work on upconversion of quantum dot single photon sources has included temporal shaping of the photon wavepackets using an amplitude modulated 1550 nm pump [12] and experiments demonstrating that two-photon interference is preserved during frequency conversion [10]. The latter work also considered the use of frequency conversion to erase spectral distinguishability by converting the light from spectrally distinct sources to a common frequency. This work was quite analogous to an experiment that preceded it by a few years [13], which converted signal and idler photons from a correlated photon pair source to a common wavelength using sum frequency generation in a pair of PPLN waveguides, and then demonstrated two-photon interference of the now spectrally indistinguishable photons.

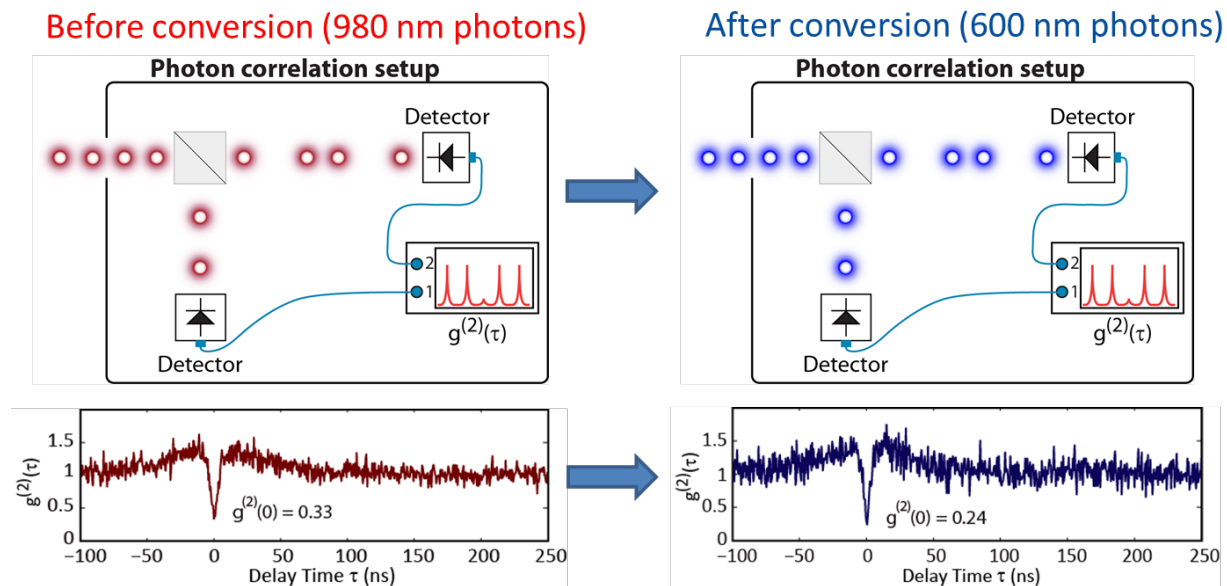


Fig. 3-2. Photon statistics measured before and after frequency upconversion, as in Ref. 10. (Top left) 980 nm photons generated by a single InAs/GaAs quantum dot pumped with a continuous-wave 780 nm laser are sent into a beamsplitter, and photons in each output port detected by a single photon counter. A histogram of coincidence counts as a function of the difference in arrival times τ between the two paths (bottom left) is generated, showing antibunching with a value $g^{(2)}(0) = 0.33 \pm 0.03$ ($g^{(2)}(\tau)$ is the normalized coincidence counting curve). (Top right) After frequency conversion to 600 nm using a 1550 nm pump in a PPLN waveguide, photons are directed into a beamsplitter, and photons in each output port are detected by a single photon counter. The generated coincidence histogram (bottom right) shows antibunching ($g^{(2)}(0) = 0.24 \pm 0.04 < 0.5$), indicating that the single photon nature of the input signal is preserved. The improved $g^{(2)}(0)$ value is likely due to the extra spectral filtering provided by the quasi-phase-matching response of the PPLN waveguide. The uncertainty in the $g^{(2)}(0)$ values is due to fluctuations in the detected photon count rate and represents a one standard deviation value.

Frequency downconversion through difference frequency generation in a $\chi^{(2)}$ medium has also been experimentally explored in the context of single photon input fields. One experiment [14] used an entangled photon pair source and demonstrated that entanglement between signal and idler photons was preserved after downconversion of one of the two fields (essentially the downconversion equivalent of the upconversion experiment of Ref. 3), as well as explicitly showing that the downconverted field exhibited antibunched photon statistics (through a heralded $g^{(2)}$ measurement). Frequency downconversion has also been demonstrated with triggered single photon sources based

on a single semiconductor quantum dot, with photon antibunching and coherence shown to be preserved [15] and downconversion to the 1550 nm band was used as an integral part of a spin-photon entanglement experiment [16].

3.2 Third-order nonlinear media

Quantum frequency conversion using the third-order nonlinear susceptibility $\chi^{(3)}$ is achieved by the process of four-wave-mixing Bragg scattering [17], sometimes referred to in the literature as wavelength exchange [18]. This is a non-degenerate four-wave-mixing process in which two pump fields create an effective modulation in the $\chi^{(3)}$ nonlinearity, enabling the (in principle) noise-free translation of an input signal to an output that is shifted by an amount equal to the difference in the two pump frequencies (Fig. 3-3). The importance of using four-wave-mixing Bragg scattering for QFC was highlighted by McKinstrie and colleagues [17]. They outlined the noise considerations that arise when considering different four-wave-mixing processes, including degenerately pumped processes, which can provide wavelength conversion but will also be accompanied by spontaneous emission noise (i.e., pump photons converted to the output wavelength band).

The dual pumps in four-wave-mixing Bragg scattering provide a great deal of flexibility in the span over which frequency conversion can take place, with both narrow and wide ranges for both upconversion and downconversion possible. Figure 3.3(b) schematically shows some of the different configurations of pumps, input signal, and output converted signal that can be utilized to achieve these different functionalities. Interestingly, it should be pointed out that for each configuration, two possible idlers can be generated, as both are energy conserving. Phase-matching then determines which idler is more efficiently generated (noting that for a long interaction length, even a small phase mismatch can be enough to select for one idler).

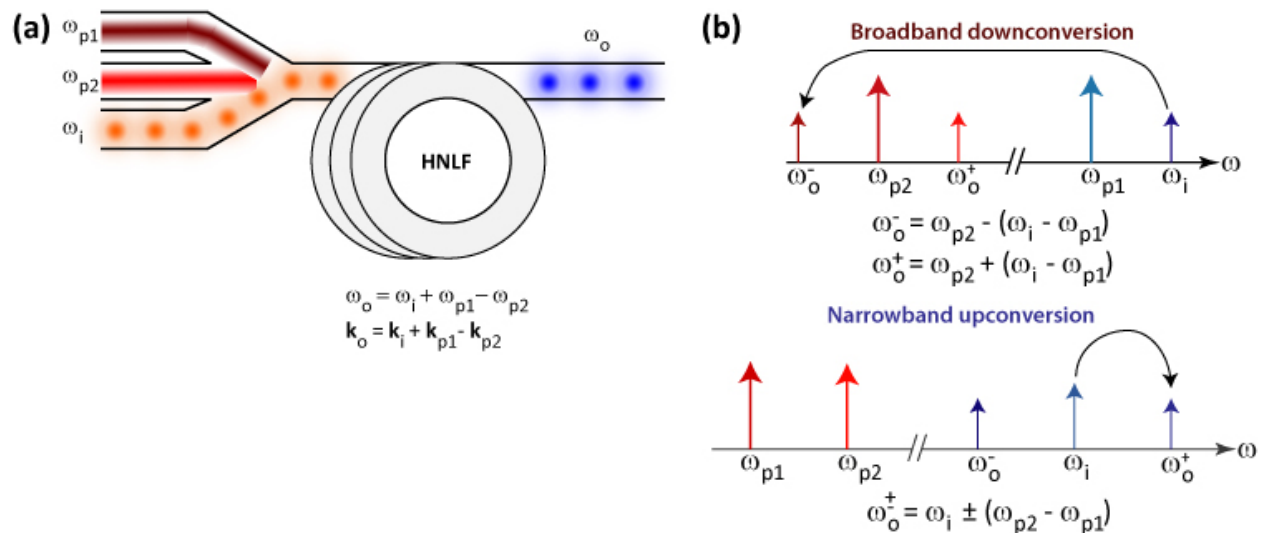


Fig. 3-3. Four-wave-mixing Bragg scattering. (a) Two strong pumps at frequencies ω_{p1} and ω_{p2} are combined with an input signal at ω_i to generate an output converted field at ω_o which, in this case, is shifted from the input by an amount $\omega_{p1} - \omega_{p2}$. (b) Different configurations for four-wave-mixing Bragg scattering. (Top) Broadband downconversion can be achieved by placing pumps ω_{p1} and ω_{p2} ($\omega_{p1} > \omega_{p2}$) in widely separated bands, with input signal ω_i at a wavelength closer to ω_{p1} than ω_{p2} ; broadband upconversion (not shown) can similarly be achieved, with input signal closer to ω_{p2} . (Bottom) Narrowband conversion can be achieved by placing pumps ω_{p1} and ω_{p2} relatively close to each other in frequency. In all of these cases, two possible idlers can be generated, consistent with energy conservation, and phase matching determines the efficiency with which each idler is produced.

The most common medium for four-wave-mixing Bragg scattering has been some form of an optical fiber, including photonic crystal fiber [19] and highly nonlinear dispersion shifted fiber [18,20,21]. Though the $\chi^{(3)}$ nonlinearity is

generally much weaker than the $\chi^{(2)}$ nonlinearity, the combination of relatively localized field confinement, the low propagation losses, and ability to fabricate optical fibers uniformly over length scales of kilometers has enabled four-wave-mixing Bragg scattering frequency converters to achieve a conversion efficiency of about 30 % for experiments at visible wavelength [19] and nearing unity in the telecommunications band [17-21] (typical length scales are ≈ 30 m for photonic crystal fiber and ≈ 1 km for highly nonlinear fiber in comparison to a few cm for lithium niobate). Phase-matching is achieved in these optical fibers by careful dispersion engineering, where waveguiding dispersion (the variation in light's phase velocity with wavelength, due to the wavelength-dependent distribution of the optical field within the fiber core and cladding) can compensate for material dispersion.

While noise-free in principle, just as in the case of sum-frequency-generation and difference-frequency-generation in $\chi^{(2)}$ media, four-wave-mixing Bragg scattering in optical fibers can be limited by a number of different possible noise sources. Spontaneous Raman scattering, a known phenomenon in silica optical fibers, can be a dominant noise source when the converted output lies relatively close in wavelength to the pumps. This has been the case in experiments in which all four fields are near the telecommunications band, as explicitly discussed in Ref. 21, where the Raman noise signal was of similar strength to the weak (single photon level) coherent state input signal. For pumps that are more widely separated from the input signal and frequency converted output, noise due to spontaneous Raman scattering is more limited [19]. Other possible noise sources can include undesired four-wave-mixing processes, which in some circumstances, could be phase-matched (or close to phase matched). For example, this could include spontaneous four-wave-mixing from one of the pumps (degenerate) or both of the pumps (non-degenerate).

Quantum frequency conversion experiments in $\chi^{(3)}$ media utilizing non-classical states of light have not been as widespread as they have in $\chi^{(2)}$ materials, with the first experiment being performed a few years ago [19]. Here, the output of a heralded single photon source produced by a photonic crystal fiber was upconverted by 24 nm to 659 nm in a second photonic crystal fiber. With input and frequency converted signals > 150 nm on the anti-Stokes (higher frequency) side of the pumps, spontaneous Raman scattering was limited and $g^{(2)}(0)$ was essentially unchanged after frequency conversion.

3.3 Future directions with quantum frequency conversion

New media and devices for quantum frequency conversion are an active area of research, spurred in part by recent work demonstrating nonlinear optical phenomena in integrated and scalable nanophotonic geometries, including some of the systems discussed earlier in this chapter. Within $\chi^{(2)}$ media, efforts at producing higher levels of device integration and more compact form factors within the lithium niobate platform have shown promise, including recent work on developing thin-film lithium niobate devices [22] and integrating them with silicon-based materials. Other $\chi^{(2)}$ media studied have included GaAs, GaP, and GaN, for which there has been work to demonstrate second harmonic generation and sum and difference frequency generation in waveguide geometries [23], as well as recent efforts to establish second harmonic generation in nanophotonic cavity geometries [24]. Though these works are currently focused on the classical domain, improvements in conversion efficiency and an understanding of potential noise mechanisms could enable QFC experiments, with future prospects including direct integration with single photon emitters based on InAs/GaAs quantum dots, for example.

Recently, four-wave-mixing Bragg scattering based on the $\chi^{(3)}$ nonlinearity in silicon nitride (Si_3N_4) waveguides fabricated on a Si substrate has been demonstrated [25], with both narrowband (few nanometers) and wideband (few hundreds of nanometers) upconversion and downconversion shown in the classical regime. Along with its broadband optical transparency and lack of two-photon absorption for pump wavelengths > 700 nm, Si_3N_4 does not appear to show significant amounts of spontaneous Raman scattering, so that early indications suggest high signal-to-noise levels can be achieved in this system. Furthermore, the combination of strong field confinement and the relatively high $\chi^{(3)}$ in Si_3N_4 create an effective nonlinearity that can be two orders of magnitude greater than that of highly nonlinear fiber. However, the relatively short Si_3N_4 waveguide length (1 cm) is in stark contrast to the typical

hundreds of meters used for QFC in fibers, and conversion efficiencies have been limited to 5 %, with all experiments done strictly in the classical regime. Chalcogenide materials such as As_2S_3 , which also has a broad optical transparency and limited two-photon absorption for pump wavelengths > 800 nm, might also be a strong candidate for four-wave-mixing Bragg scattering, particularly due to its higher nonlinear refractive index $n_2 = 2.4$. Silicon is also a possibility for certain applications (e.g., telecom), particularly if pump wavelengths > 2.0 μm can be used to avoid two-photon absorption, as has recently been demonstrated for degenerate four-wave-mixing experiments [26].

Over the past few years, there have been a number of works looking to extend QFC from only shifting the color of quantum states of light to also providing temporal wavepacket shaping [5], a necessary resource for many applications in photonic quantum information science. For example, optimal storage of a single photon in a quantum memory will generally require control of not only the wavelength but also the spectro-temporal profile of the photon. Frequency conversion provides a versatile route to wavepacket shaping in large part because the nature of the process is such that the frequency converted field has characteristics that depend both on the input signal (a quantum field) and the input pump field(s) (strong classical field(s)). An early example of this was demonstrated experimentally in Ref. [12], where classical pump pulses were used to produce upconverted single photons of a controllable duration (in the regime where the pump pulses were shorter than the input single photon pulses). That work essentially applied a nonlinear time gating operation to the input single photon states, and was therefore not lossless (even in principle).

There has been much progress on the theoretical front in developing lossless protocols for full spectro-temporal shaping of quantum light fields. In Ref. [27], a two-step process was proposed. The first step consists of spectral broadening and shaping of a single photon wavepacket through nonlinear mixing with a classical pump that has been imprinted with a specified temporal phase. The output single photon wavepacket has the desired frequency spectrum, and the spectral phase can then be corrected (using classical pulse shaping approaches) to allow for full temporal shaping. This approach could be used to strongly compress single photon pulses produced by single quantum emitters, which often have nanosecond (or longer) time constants. In Ref. [28], engineering of the group velocities of the pump and input signal in a $\chi^{(2)}$ medium was considered as a means to either compress or stretch a single photon wavepacket, depending on whether the pump moves faster or slower than the input signal. Single photon wavepacket shaping using four-wave-mixing Bragg scattering has also been considered [29,30], with a recent result [30] showing an arbitrary input field temporal profile can be mapped to an arbitrary output field profile with unity efficiency. In comparison to the previous work [29], in which there was a tradeoff between selectivity (ability to map the input to only one desired output) and efficiency, Ref. 30 provides a prescription for providing perfect (in principle) selectivity and efficiency.

References

- [1] P. Kumar, "Quantum Frequency Conversion," *Optics Letters*, **15**(24), 1476-1478 (1990).
- [2] J. Huang and P. Kumar, "Observation of Quantum Frequency Conversion," *Physical Review Letters*, **68**(14), 2153-2156 (1992).
- [3] S. Tanzilli et al, "A photonic quantum interface," *Nature*, **437**, 116-120 (2005).
- [4] A.P. VanDeVender and P.G. Kwiat, "High efficiency single photon detection via frequency up-conversion," *Journal of Modern Optics*, **51**(9-10), 1433-1445 (2004); M. Albota and F. Wong, "Efficient single-photon counting at 1.55 μm by means of frequency upconversion," *Optics Letters*, **29**(13), 1449-1451 (2004).
- [5] M.G. Raymer and K. Srinivasan, "Manipulating the color and shape of single photons," *Physics Today*, **65**(11), 32-37 (2012).
- [6] M.M. Fejer, "Nonlinear Optical Frequency Conversion," *Physics Today*, **47**(5), 25-32 (1994).
- [7] C. Langrock et al., "Highly efficient single-photon detection at communication wavelengths by use of upconversion in reverse-proton-exchanged periodically poled LiNbO_3 waveguides," *Optics Letters*, **30**(13), 1725-1727 (2005).
- [8] J.S. Pelc et al, "Long-wavelength-pumped upconversion single-photon detector at 1550nm: performance and noise analysis," *Optics Express*, **19**(22), 21445-21456 (2011).

- [9] J.S. Pelc et al, "Influence of domain disorder on parametric noise in quasi-phase-matched quantum frequency converters," *Optics Letters*, **35**(16), 2804-2806 (2010).
- [10] S. Ates et al, "Two-Photon Interference Using Background-Free Quantum Frequency Conversion of Single Photons Emitted by an InAs Quantum Dot," *Physical Review Letters*, **109**, 147405 (2012).
- [11] M.T. Rakher et al, "Quantum transduction of telecommunications-band single photons from a quantum dot by frequency upconversion," *Nature Photonics*, **4**, 786-791 (2010).
- [12] M.T. Rakher et al, "Simultaneous Wavelength Translation and Amplitude Modulation of Single Photons from a Quantum Dot," *Physical Review Letters*, **107**, 083602 (2011).
- [13] H. Takesue, "Erasing distinguishability using quantum frequency conversion," *Physical Review Letters*, **101**, 173901 (2008).
- [14] R. Ikuta et al, "Wide-band quantum interface for visible-to-telecommunication wavelength conversion," *Nature Communications*, **2**(537), 1544-1548 (2011).
- [15] S. Zaske et al, "Visible-to-telecom quantum frequency conversion of light from a single quantum emitter," *Physical Review Letters*, **109**, 147404 (2012).
- [16] K. De Greve et al, "Quantum-dot spin-photon entanglement via frequency downconversion to telecom wavelength," **491**, 421-425 (2012).
- [17] C.J. McKinstrie et al, "Translation of quantum states by four-wave-mixing in fibers," *Optics Express*, **13**(22), 9131-9142 (2005).
- [18] K. Uesaka et al, "Wavelength Exchange in a Highly Nonlinear Dispersion-Shifted Fiber: Theory and Experiments," *IEEE J. Selected Topics in Quantum Electronics*, **8**(3), 560-568 (2002).
- [19] H.J. McGuinness et al, "Quantum Frequency Translation of Single-Photon States in a Photonic Crystal Fiber," *Physical Review Letters*, **105**, 093604 (2010).
- [20] A.H. Gnauck et al, "Demonstration of low-noise frequency conversion by Bragg scattering in a fiber," *Optics Express*, **14**(20), 8989-8994 (2006).
- [21] A.S. Clark et al, "High-efficiency frequency conversion in the single-photon regime," *Optics Letters*, **38**(6), 947-949 (2013).
- [22] A. Guarino et al, "Electro-optically tunable microring resonators in lithium niobate," *Nature Photonics*, **1**, 407-410 (2007).
- [23] L. Lanco et al, "Backward difference frequency generation in an AlGaAs waveguide," *Applied Physics Letters*, **89**, 031106 (2006); J. Han et al, "Continuous-wave sum-frequency generation in AlGaAs Bragg reflection waveguides," *Optics Letters*, **34**(23), 3656-3658 (2009).
- [24] K. Rivoire et al, "Second harmonic generation in gallium phosphide photonic crystal nanocavities with ultralow continuous wave pump power," *Optics Express*, **17**(25), 22609-22615 (2009); C. Xiong et al, "Integrated GaN photonic circuits on silicon (100) for second harmonic generation," *Optics Express*, **19**(11), 10462-10470 (2011); Y. Ota et al, "Nanocavity-based self-frequency conversion laser," *Optics Express*, **21**(17), 19778-19789 (2013); P.S. Kuo, J. Bravo-Abad, and G.S. Solomon, "Second-harmonic generation using quasi-phasematching in a GaAs whispering-gallery-mode microcavity," *Nature Communications*, **5**, 3109 (2014).
- [25] I.H. Agha et al, "Low-noise chip-based frequency conversion by four-wave-mixing Bragg scattering in SiN_x waveguides," *Optics Letters*, **37**(14), 2997-2999 (2012); I.H. Agha et al, "A chip-scale, telecommunications-band frequency conversion interface for quantum emitters," *Optics Express*, **21**(18), 21628-21638 (2013).
- [26] X. Liu et al, "Mid-infrared optical parametric amplifier using silicon nanophotonic waveguides," *Nature Photonics*, **4**, 557-560 (2010); S. Zlatanovic et al, "Mid-infrared wavelength conversion in silicon waveguides using ultracompact telecom-band-derived pump source," *Nature Photonics*, **4**, 561-564 (2010).
- [27] D. Kielpinski et al, "Quantum optical waveform conversion," *Physical Review Letters*, **106**, 130501 (2011).
- [28] B. Brecht et al, "From quantum pulse gate to quantum pulse shaper – engineered frequency conversion in nonlinear optical waveguides," *New Journal of Physics*, **13**, 065029 (2011).
- [29] C.J. McKinstrie et al, "Quantum-state-preserving optical frequency conversion and pulse reshaping by four-wave-mixing," *Physical Review A*, **85**, 053829 (2012).
- [30] D.V. Reddy et al, "Efficient sorting of quantum-optical wavepackets by temporal-mode interferometry," *Optics Letters*, **39**(10), 2924-2927 (2014).